Electronic Research Archive

http://www.aimspress.com/journal/era

ERA, 32(3): 2203–2228.
DOI: 10.3934/era.2024100
Received: 12 December 2023
Revised: 07 February 2024
Accepted: 27 February 2024
Published: 18 March 2024

Research article

A non-autonomous time-delayed SIR model for COVID-19 epidemics prediction in China during the transmission of Omicron variant

Zhiliang Li[1], Lijun Pei[1,*], Guangcai Duan[2] and Shuaiyin Chen[2]

[1] School of Mathematics and Statistics, Zhengzhou University, Henan 450001, China
[2] School of Public Health, Zhengzhou University, Henan 450001, China

* **Correspondence:** Email: peilijun@zzu.edu.cn; Tel: +8637167783167.

Abstract: With the continuous evolution of the coronavirus, the Omicron variant has gradually replaced the Delta variant as the prevalent strain. Their inducing epidemics last longer, have a higher number of asymptomatic cases, and are more serious. In this article, we proposed a nonautonomous time-delayed susceptible-infected-removed (NATD-SIR) model to predict them in different regions of China. We obtained the maximum and its time of current infected persons, the final size, and the end time of COVID-19 epidemics from January 2022 in China. The method of the fifth-order moving average was used to preprocess the time series of the numbers of current infected and removed cases to obtain more accurate parameter estimations. We found that usually the transmission rate $\beta(t)$ was a piecewise exponential decay function, but due to multiple bounces in Shanghai City, $\beta(t)$ was approximately a piecewise quadratic function. In most regions, the removed rate $\gamma(t)$ was approximately equal to a piecewise linear increasing function of (a*t+b)*H(t-k), but in a few areas, $\gamma(t)$ displayed an exponential increasing trend. For cases where the removed rate cannot be obtained, we proposed a method for setting the removed rate, which has a good approximation. Using the numerical solution, we obtained the prediction results of the epidemics. By analyzing those important indicators of COVID-19, we provided valuable suggestions for epidemic prevention and control and the resumption of work and production.

Keywords: SIR; predictions; COVID-19; Omicron; China

1. Introduction

The Omicron variant is a mutated form of the Delta variant, characterized by its greater transmissibility, shorter incubation period, higher viral load, and increased ability to evade the immune system. As a result, the rate of severe illness is on the decrease and most infected individuals are asymptomatic. Some old people infected by the Omicron variant are in danger due to poor immune systems and other

previous diseases. The surge in the number of infected people can overwhelm medical resources, resulting in inadequate care and increased mortality rates. Additionally, the workforce may be impacted, leading to disruptions in various sectors. China detected the Omicron virus in individuals entering the country as early as December 2021. On January 8th, 2022, China's first confirmed case was reported in Tianjin, where the number of accumulative infected cases reached 406 after 12 days. The transmission of the virus occurred when a university student studying in Tianjin returned to Anyang in Henan Province, causing widespread transmission in Anyang City and Tangyin County. Up to January 19th, 2022, the number of infected cases in Tangyin County had exceeded 400. The first Omicron case was detected in Beijing on January 15th, 2022. He was infected via international mail. On March 1st, Yanbian Prefecture in Jilin Province, Qingdao City in Shandong Province, and Putuo District in Shanghai reported their first confirmed cases on the same day. Then, in Shandong, Guangdong, Hebei, Yunnan Provinces, Shanghai City and other places, the Omicron variant spread rapidly, and the number of infected people increased sharply. The epidemic situation worsened rapidly.

Some genetic mutations occurred in the important genetic locus of the Omicron variant, which made the COVID-19 vaccine more difficult to defend against the Omicron [1–3]. In the 1920s, Kermack and McKendrick [4] proposed the original SIR (Susceptible-Infected-Removed) model, from which many variants of the SIR model were derived. In 1979, the time-delayed epidemic model was proposed [5]. Guglielmi et al. [6] introduced the delay differential equation epidemic model and conducted some experiments. The time-delayed SIR model was used to study the COVID-19 epidemic in Italy [7]. Rahimi et al. [8] detailedly introduced some models and algorithms used for COVID-19 prediction. Lv et al. [9] proposed the time-delayed SAIR (Susceptible-Asymptomatic-Infected-Recovered) model to study the time of the booster vaccination against COVID-19, and found 6 months to be the best time. Mohamadou et al. [10] introduced artificial intelligence, datasets, and mathematical modeling of the COVID-19 epidemic. Inverse problem solving methods were used to solve for transmission and removed rates, which are functions of time [11]. The numerical solution and systems theory was applied to study the transmission rate [12]. The parameter calibration of the SIR model was discussed [13]. Cooper et al. [14] applied a SIR model to analyze the developments of COVID-19 epidemics in some communities and provide some valuable viewpoints on epidemic prevention and control. Inverse reliability approach and the differential evolution algorithm were used to estimate the parameters of the SIRD (Susceptible-Infectious-Recovery-Dead) model [15]. The Levenberg–Marquardt algorithm and Tikhonov regularization were applied to estimate the parameters of the SIRD model [16]. The influence of uncertainty in the design variables was considered [17]. Nonautonomous delayed SIR and SIRD models can be used for making long-term predictions in China [18–20]. Jahanshahi et al. [21] adopted a fractional-order SIRD model based on the Caputo derivative for incorporating the memory effects to analyze the developments of the COVID-19 epidemic. Anastassopoulou et al. [22] evaluated the mortality and cure rates based on the previous data and then used the SIRD model to predict the COVID-19 epidemic in Wuhan City, China. Some scholars applied the SEIR (Susceptible-Exposed-Infected-Removed) model to the early prediction of COVID-19 and obtained some meaningful results [23–28]. Fan and Li [29] considered the environmental transmission model to analyze the COVID-19 epidemic. The eSIR (extended susceptible-infected-removed) model with Markov Chain Monte Carlo methods was applied to predict the trend in Italy and Hunan Province, China [30]. Based on the weak immunity provided by the vaccine, Turkyilmazoglu [31] proposed an extension of the SIR model to the SIRVI (S-Susceptible, I-Infected I, V-Vaccinated, and R-Removed/Recovered) model.

The Boosted Random Forest algorithm was adopted to predict the COVID-19 epidemic [32]. Machine learning combined with artificial intelligence algorithms has been widely employed to forecast various indexes of COVID-19 epidemics [33–36]. Salgotra et al. [37] proposed GEP (Genetic Evolutionary Programming) based models to analyze the possible impact of the COVID-19 epidemic and predict future cases in India. Abbasimehr and Paki [38] combined multi-head attention, LSTM (Long Short-Term Memory), and CNN (Convolutional Neural Network) with the Bayesian optimization algorithm to forecast the COVID-19 epidemic. Turkyilmazoglu [39] studied the peak formula of the traditional SIR model without numerical simulation, which can reduce the computational time and cost. Turkyilmazoglu [40] further optimized the peak formula to obtain a more accurate and simpler formula and addressed some shortcomings. Some experimental results are presented in [40].

In the above papers, several excellent models and methods for forecasting the COVID-19 epidemic were presented. However, some scholars did not take into account the impact of incubation, which is a crucial factor affecting the accuracy of COVID-19 predictions. Therefore, in this article, we propose a NATD-SIR (nonautonomous time-delayed) model for COVID-19 epidemics prediction during the transmission of the Omicron variant. Compared with [18], we have made several improvements to better predict the COVID-19 epidemic during the transmission of the Omicron variant. To improve the accuracy of predictions, we adopt the fifth-order moving average method to preprocess the data, which helps to smooth the data, avoiding the interference of extreme values and enhancing prediction accuracy. Through the finite difference method, we find that $\beta(t)$ is approximately equal to an exponential decay function in most epidemics induced by the Omicron variant. However, due to the highly contagious nature of the Omicron variant, the COVID-19 epidemic situation becomes more complicated. The transmission rates in the initial days exhibit significant variation, which adversely affects the estimation of overall transmission rates. Hence, we adopt a piecewise exponential decay function to estimate the transmission rates. Through our experiments, the transmission rate of the piecewise exponential decay function greatly improves the prediction accuracy for the epidemic induced by the Omicron variant compared to the transmission rate of the exponential decay function. Specifically, in Shanghai City, where multiple bounces occurred in the COVID-19 epidemic, the transmission rate is modeled as a piecewise quadratic function rather than an exponential decay function. In addition, $\gamma(t)$ is approximately (a*t+b)*H(t-k) (a>0), but $\gamma(t)$ is approximately c*exp(dt)*H(t-k) (c>0, d>0) in a few epidemics induced by the Omicron variant. In addition, [18] does not do a good job of explaining how the removed rates are set when the removed persons are zero in the data we use for parameter estimation. In practice, there will be no removed persons in the first few days, so we need to solve this problem in order to predict the COVID-19 epidemic earlier and more accurately. The first removed case appears at different time, roughly the 18th day. When we estimate the parameters of transmission and removed rates by using data from the initial few days, the number of removed persons is sometimes too small or even zero, making it challenging to estimate the parameters accurately. We need to set removed rates, which refers to the removed rates in [18], where the removed rates of epidemics induced by the Delta variant in Putian with a small population of 3.2107 million people and Harbin City with a large population of 10.0099 million people are (0.003t+0.01)*H(t-14) and (H(t-14))*(0.005 *t+0.02), respectively. In [18], the numbers of accumulative infected persons in Putian and Harbin are 204 and 88. In the regions whose population is close to Putian or Harbin cities, in that the accumulative number of infected persons is far more than that in Putian or Harbin, we set the removed rates as (H(t-18))*(0.002 t+0.01) or (H(t-18))*(0.004 t+0.02), respectively. We bring the parameters of trans-

mission and removed rates estimated by the first ten days or more into the model to make long-term predictions. The predicted results are consistent with the actual results. We obtain the maximum number of current infected persons, the time at which it occurs, the final size of the COVID-19 epidemic, and the end time of the epidemic. Based on these predictions, we can provide the governments with effective epidemic control measures.

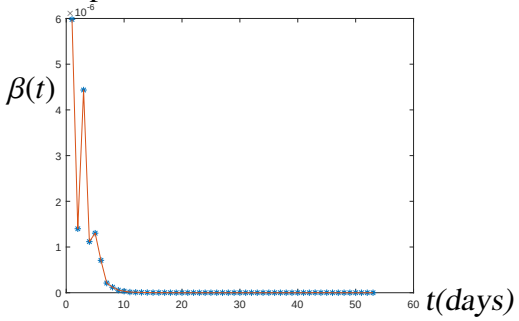

(a) Binzhou City

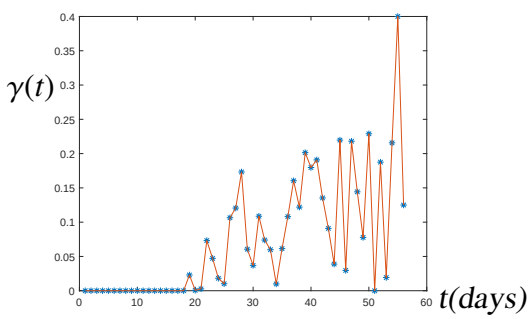

(b) Binzhou City

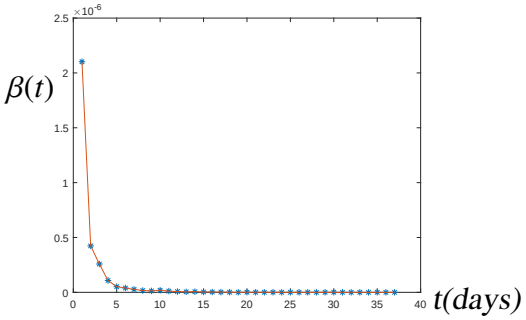

(c) Quanzhou City

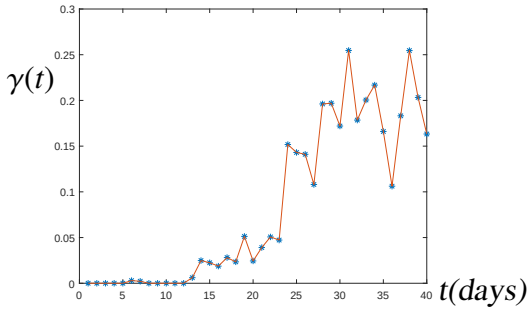

(d) Quanzhou City

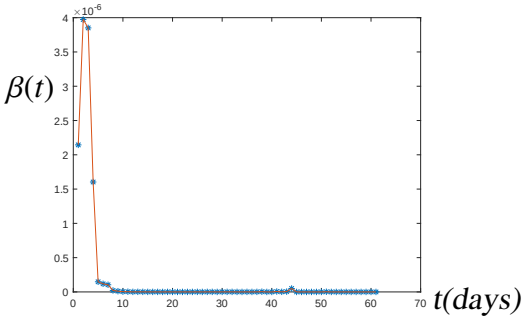

(e) Qingdao City

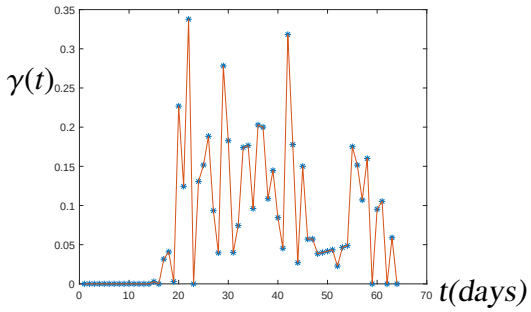

(f) Qingdao City

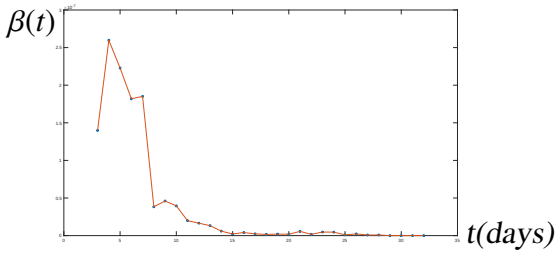

(g) Harbin City 1

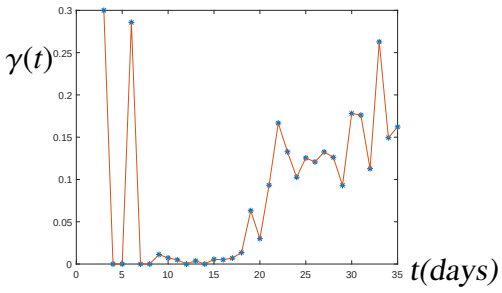

(h) Harbin City 1

Continued on next page

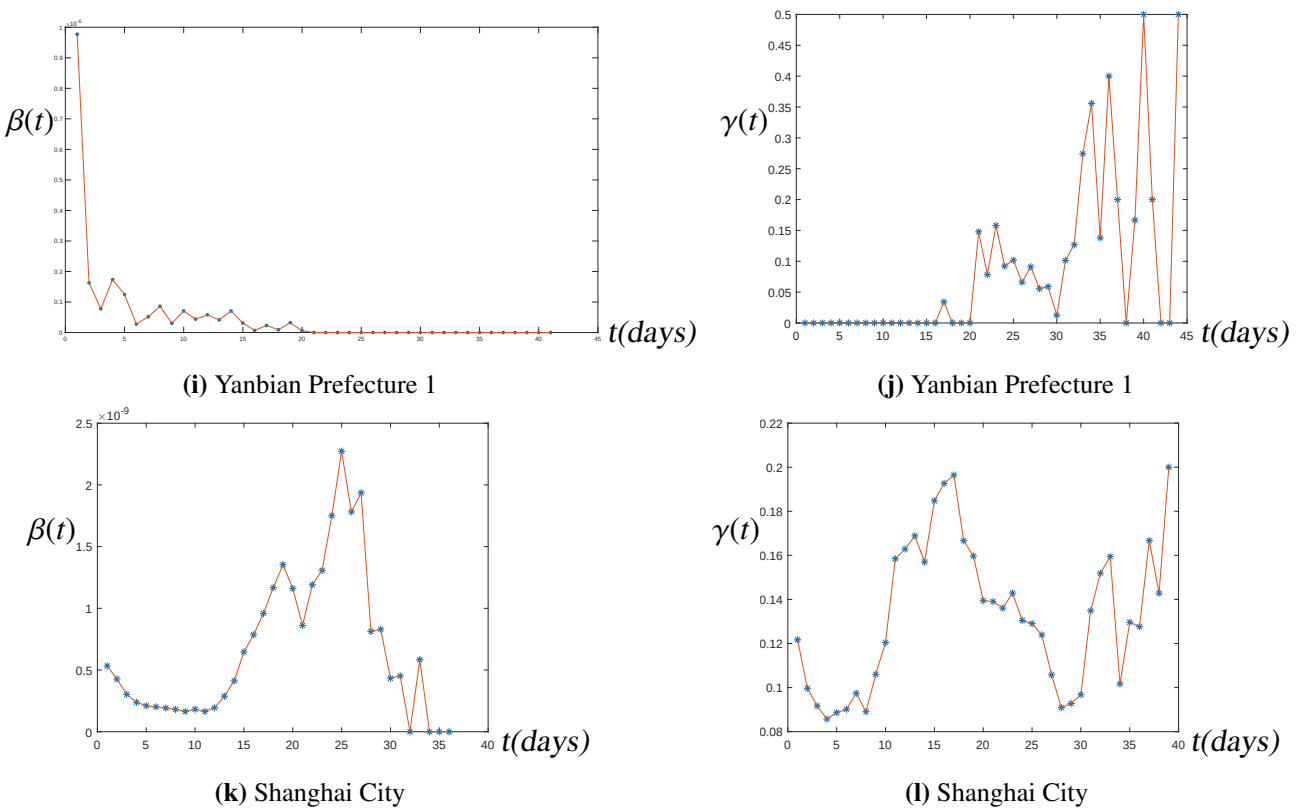

(i) Yanbian Prefecture 1 **(j)** Yanbian Prefecture 1

(k) Shanghai City **(l)** Shanghai City

Figure 1. Transmission rates and removed rates in Binzhou City (1a-1b), Quanzhou City(1c-1d), Qingdao City (1e-1f), Harbin City 1(1g-1h), Yanbian Prefecture 1(1i-1j), and Shanghai City (1k-1l).

This article has the following structure. An NATD-SIR model is introduced in Section 2. In Section 3, we present the sources of COVID-19 data of the relevant regions. In Section 4, predictions of small-scale COVID-19 epidemics during the transmission of the Omicron variant are presented. In Section 5, predictions of large-scale COVID-19 epidemics during the transmission of the Omicron variant are presented. In Section 6, we present the conclusions and discussion.

2. Description of an NATD-SIR model

In this article, we adopt an NATD-SIR model to predict the current susceptible, infected, and removed persons in COVID-19 epidemics during the transmission of the Omicron variant. It is based on the following assumptions. First, we don't take into account the demographic dynamics, i.e., birth and death rates. Second, the whole population is a constant, i.e., $S(t) + I(t) + R(t) \equiv N$. The following symbols represent the numbers of the current susceptible persons, infected persons, and the accumulative removed persons:

S(t): The current susceptible persons, standing for the number of the group who is not infected but is at risk of infection at time t.

I(t): The current infected persons, standing for the number of confirmed and asymptomatic infected

patients at time t.

R(t): The accumulative removed persons, standing for the accumulative number of the recovered persons, the asymptomatic persons who are released from observation, and dead persons at time t.

There are some highlights in this model.

First, we take into account the impact of the incubation period of the Omicron variant. The incubation period refers to the period during which pathogens enter into the body but no clinical symptom appears. If typical symptoms appear, the individual will take a nucleic acid test and become a confirmed case. We assume the incubation period of τ days. In mainland China, asymptomatic persons also take τ days to be detected and become asymptomatic infected patients due to nucleic acid testing and quarantine measures for close contacts. The average incubation period is not consistent for different COVID-19 viruses. [41] showed that the mean incubation period of 3.4 days for the Omicron variant was shorter than 3.8 days for the Delta variant. We rounded up the value of the mean incubation period. We set the mean incubation period for the Delta variant to be 4 days and for the Omicron variant to be 3 days. For COVID-19 epidemics prediction, the influence of the incubation period on the accuracy of predicted results is significant. Second, based on COVID-19 data released by regional health committees, we find that transmission and removed rates are functions of time t. The transmission rates of the first few days in the target places except for Shanghai City roughly conform to the exponential decay function, but roughly fluctuate greatly. Therefore, the transmission rates from the first few days are not suitable for long-term prediction. To reduce the interference of the previous transmission rates, we set $\beta(t)$ as a piecewise exponential decay function, which is $a*\exp(b*t)*H(k-t)+c*\exp(d*t)*H(t-k)$. As the epidemics fluctuate and bounce back in Shanghai City, we set $\beta(t)$ as a piecewise quadratic function, which is $(k_1t^2+k_2t+k_3)*H(a_1-t)+(k_4t^2+k_5t+k_6)*heavisde(t-a_1)*H(a_2-t)$. In most regions, $\gamma(t)$ is approximately (a*t+b)*H(t-k) (a>0), but in a few areas, $\gamma(t)$ is approximately $c*\exp(d*t)*H(t-k)$ (c>0, d>0).

In our research, the NATD-SIR model is presented as follows:

$$\begin{aligned}
\frac{\mathrm{d}S}{\mathrm{d}t} &= -\beta(t)S(t-\tau)I(t-\tau),\\
\frac{\mathrm{d}I}{\mathrm{d}t} &= \beta(t)S(t-\tau)I(t-\tau)-\gamma(t)I(t),\\
\frac{\mathrm{d}R}{\mathrm{d}t} &= \gamma(t)I(t),
\end{aligned} \tag{2.1}$$

where $\gamma(t)$ stands for the removed rate from infected persons to removed persons and $\beta(t)$ stands for the transmission rate from susceptible persons to infected persons. By applying the finite difference method [19] to Eq (2.1), we can get the expressions of $\beta(t)$ and $\gamma(t)$ as follows:

$$\begin{aligned}
\beta(t) &\approx \frac{S(t)-S(t+1)}{S(t-\tau)I(t-\tau)},\\
\gamma(t) &\approx \frac{R(t+1)-R(t)}{I(t)}.
\end{aligned} \tag{2.2}$$

Transmission and removed rates in Binzhou City, Quanzhou City, Qingdao City, Shanghai City, Harbin City 1, and Yanbian Prefecture 1 are presented in Figure 1. Figure 1 indicates that transmission and removed rates are consistent with our analysis.

Table 1. Parameter estimations for Binzhou City, Quanzhou City, Qingdao City, Harbin City 1, and Yanbian Prefecture 1.

	$\beta(t)$	$\gamma(t)$
Binzhou City	$(H(8-t))*0.00000344240$ $*\exp(-0.40880512899t)+$ $(H(t-8))*0.00004049586$ $*\exp(-0.53292537370t)$	$(H(t-19))*(0.00597965516t$ $-0.09611988790)$
Quanzhou City	$(H(7-t))*0.00000087653$ $*\exp(-0.30279555184t)+$ $(H(t-7))*0.00000035354$ $*\exp(-0.25078571150t)$	$(H(t-12))*(0.01076807306t$ $-0.15633186938)$
Qingdao City	$(H(5-t))*0.00000074476$ $*\exp(-0.41361481767t)$ $+(H(t-5))*0.00000584764$ $*\exp(-0.49240975914t)$	$(H(t-15))*(0.01686286913t$ $-0.24732814186)$
Harbin City 1	$(H(4-t))*0.00000022532$ $*\exp(-0.0196120217t)$ $+(H(t-4))*0.00000090747$ $*\exp(-0.26163353282t)$	$(H(t-18))*(0.00748215344t$ $-0.07271696079)$
Yanbian Prefecture 1	0.00000043822 $*\exp(-0.15906181835t)$	$(H(t-18))*0.00869453706$ $-0.12337982446)$

According to the nonlinear least square method and the solution of the delayed differential equation, we get the parameter estimations of the transmission and the removed rates in Table 1, and the fitting curves of the epidemics induced by the Omicron variant in Binzhou City, Quanzhou City, Qingdao City, Harbin City 1, and Yanbian Prefecture 1. Because the number of susceptible persons is in the millions or more, the rate of transmission is very small. Also, as the nonlinear dynamical system, the delayed SIR model is sensitive to small changes in parameters. We need to keep as many bits as possible to ensure accurate parameters and further accurate predictions. The fitting curves in Figure 2 are close to the actual data. By our method, if the estimated parameters by the epidemic data of the first few days are consistent with those by the fitting of the total epidemic data, then we can accurately predict the rest of the epidemic. The reason is that since we have obtained the accurate functional forms of the total transmission and removed rates empirically, and by the few initial data, we can get these accurate rates, so after substituting them and the initial data into and simulating these delayed SIR models, we can get their accurate long-term evolution. The paramteres are more accurate, and the numerical solutions of the delayed differential equations will be more accurate. Actually, it is a question of parameters eastimation and numerical simulation for delayed differential equations, so our main work is to estimate the accurate transmission and removed rates from the initial period of the

epidemic. The model can be used to predict the COVID-19 epidemic. The experimental process of this study is shown in Figure 3.

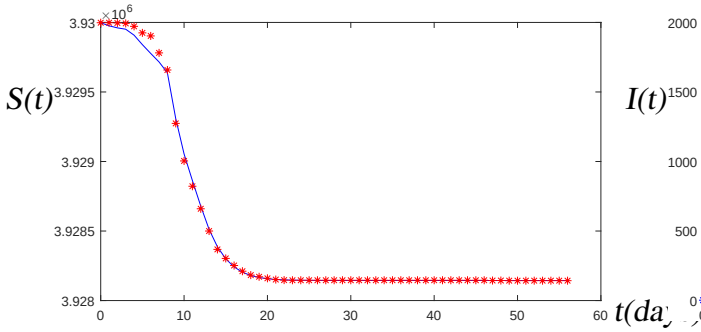

(a) Binzhou City

∗ real data - Numerical simulation

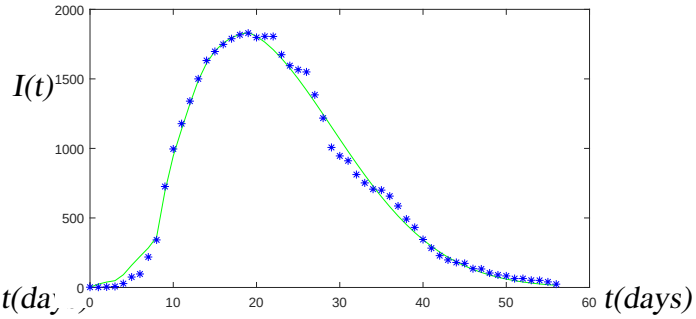

(b) Binzhou City

∗ real data - Numerical simulation

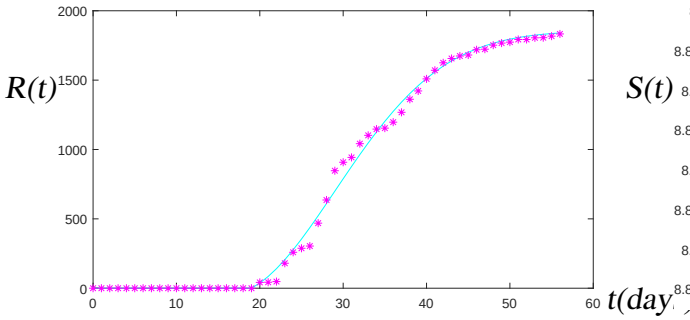

(c) Binzhou City

∗ real data - Numerical simulation

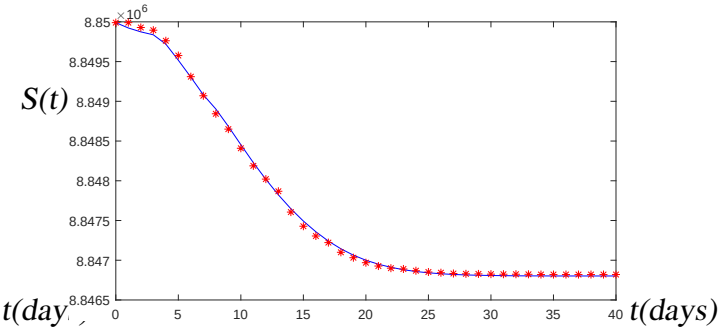

(d) Quanzhou City

∗ real data - Numerical simulation

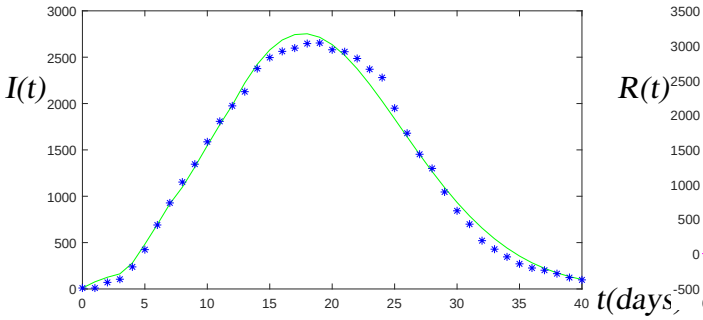

(e) Quanzhou City

∗ real data - Numerical simulation

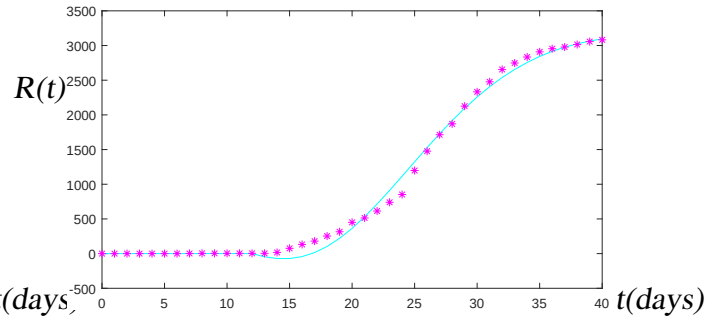

(f) Quanzhou City

∗ real data - Numerical simulation

Continued on next page

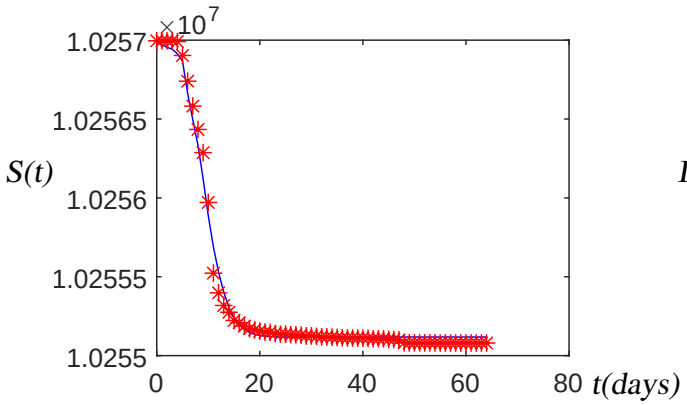

(g) Qingdao City

∗ real data - Numerical simulation

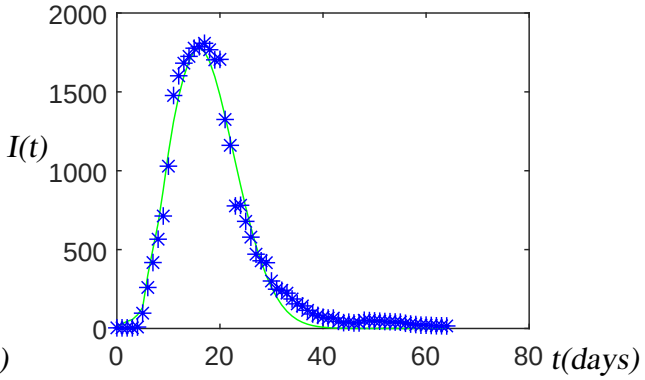

(h) Qingdao City

∗ real data - Numerical simulation

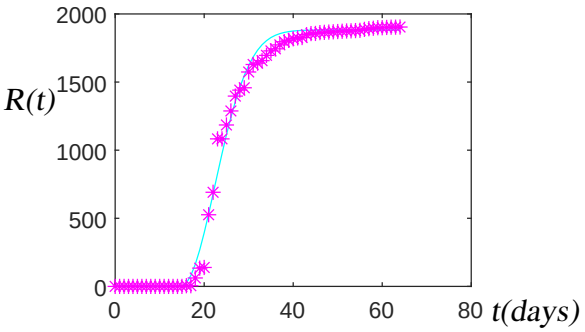

(i) Qingdao City

∗ real data - Numerical simulation

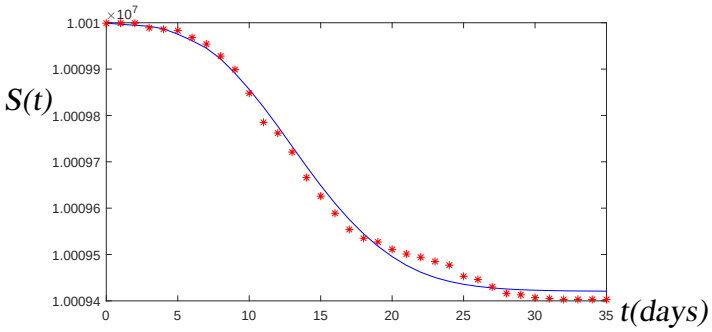

(j) Harbin City 1

∗ real data - Numerical simulation

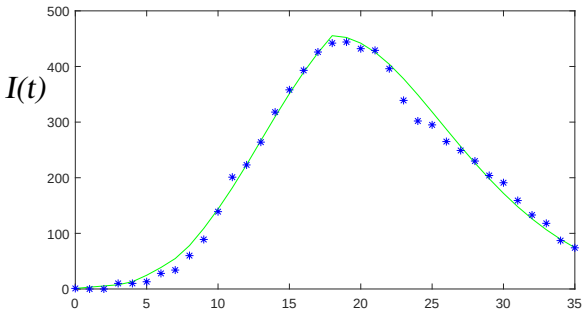

(k) Harbin City 1

∗ real data - Numerical simulation

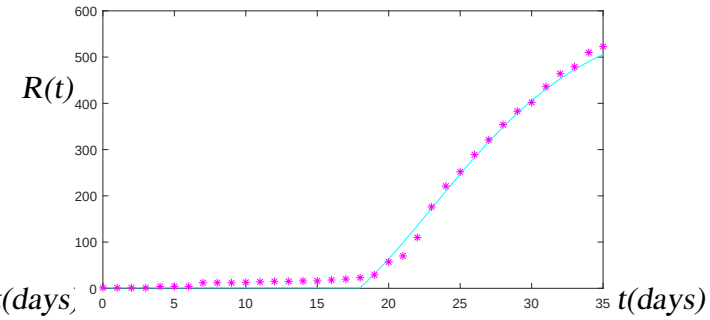

(l) Harbin City 1

∗ real data - Numerical simulation

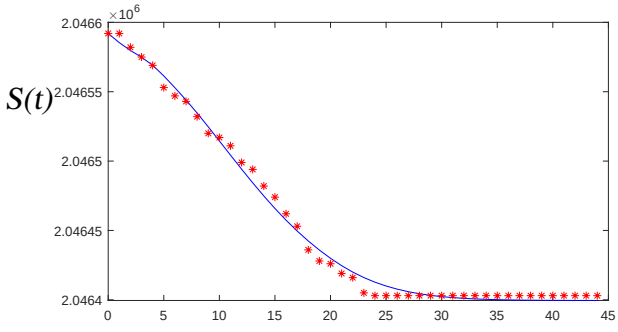

(m) Yanbian 1

∗ real data - Numerical simulation

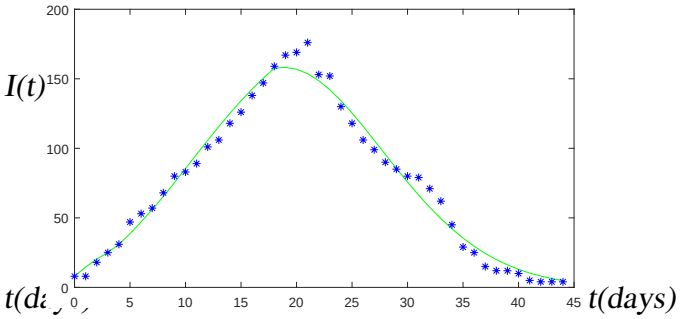

(n) Yanbian 1

∗ real data - Numerical simulation

Continued on next page

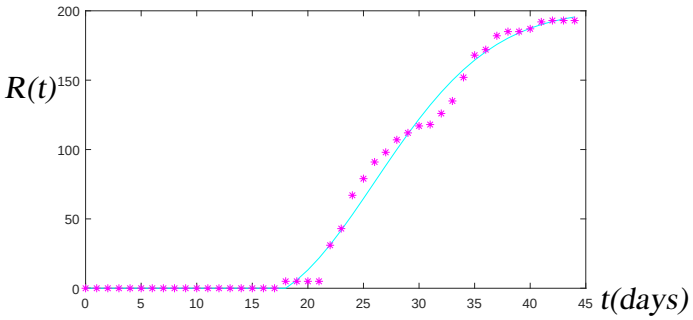

(o) Yanbian 1

$*$ real data - Numerical simulation

Figure 2. The fitting results of COVID-19 epidemics in Binzhou City (2a–2c), Quanzhou City (2d–2f), Qingdao City (2g–2i), Harbin City 1(2j–2l), and Yanbian Prefecture 1(2m–2o).

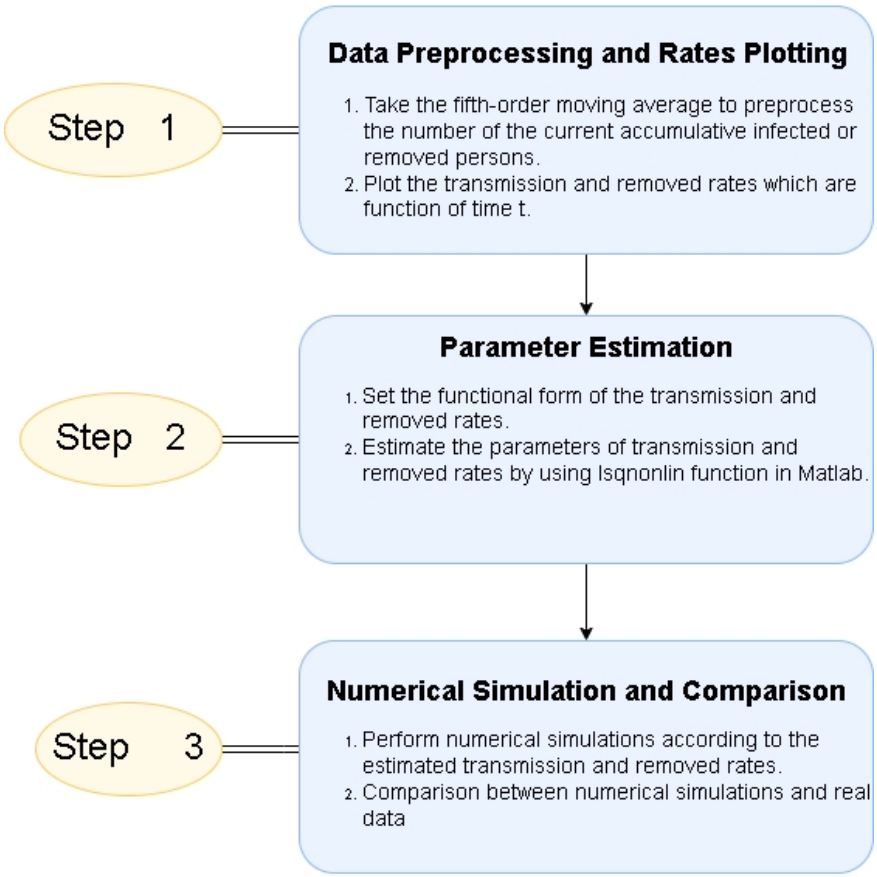

Figure 3. Flowchart.

3. Data sources

The collected data on COVID-19 comes from each regional health commission, which publishes daily local COVID-19 data. These datasets are objective and realistic. We collect data from the following website. Quanzhou City: https://wjw.fujian.gov.cn/ztzl/gzbufk/yqtb/; Qingdao City: http://wsjkw.qingdao.gov.cn/ztzl/xgfyyqfk/yqxx; Jilin City: http://www.jl.gov.cn/szfzt/jlzxd/yqtb/; Siping City: http://www.siping.gov.cn/zw/zt/yqfk/yqdt; Yanbian Prefecture: http://www.yanbian.gov.cn/zw/zt/yqfk/index_28.html; Hohhot City: http://wjw.huhhot.gov.cn/zwdt/yqfkdt/index_26.html; Binzhou City: http://wjw.binzhou.gov.cn/col/col164815/index.html; Shanghai City: https://wsjkw.sh.gov.cn/yqtb/index.html; Harbin City: http://wsjkw.hlj.gov.cn/wsjkw/c109116/zfxxgk.shtml; National Health Commission: http://www.nhc.gov.cn/xcs/yqtb/list_gzbd.shtml.

4. Predictions of small-scale COVID-19 epidemics during the transmission of the Omicron variant in China

Table 2. Start times and end times for the COVID-19 epidemics in Yanbian Prefecture and Sping, Harbin, and Hohhot cities.

	Siping City	Yanbian Prefecture 1	Yanbian Prefecture 2	Harbin City 1	Harbin City 2	Hohhot City
Start time	March 12th, 2022	March 1st, 2022	April 15th, 2022	March 8th, 2022	April 13th, 2022	February 15th, 2022
End time	April 18th, 2022	March 24th, 2022	April 28th, 2022	April 8th, 2022	May 7th, 2022	March 11th, 2022
Epidemic Strain	Omicron Variant	Omicron Variant	Omicron Variant	Omicron Variant	Omicron Variant	Delta Variant

Epidemics induced by the Omicron variant tend to last longer due to its increased infectiousness. The most critical factor for accurate epidemic prediction is accurate estimation of transmission and removed rates. The small amount of initial data will make it difficult to estimate accurate transmission and removed rates. Therefore, we need more data to be able to estimate accurate transmission and removed rates for long-term prediction. In individual regions, the first wave of epidemics came to an end, only to experience a sudden rebound and trigger a second wave. The transmission rate is an exponential decay function that gradually tends to zero over time. Toward the end of the first wave, the number of susceptible people was no longer decreasing. We should predict the two waves separately. For the second wave, we take into account the impact of the first wave. Therefore, we need to predict these two waves separately. We select Siping City, Yanbian Prefecture, and Harbin City to predict sporadic epidemics induced by the Omicron variant. Our methods and procedures go as follows.

For epidemics prediction in Siping City, we select data from the first seventeen days for parameter estimations. $\beta(t)$ is set as a piecewise exponential decay function, which is $a * \exp(b * t) * (H(14 - t)) + c * \exp(d * t) * (H(t - 14))$. Since the first removed person occurred on the 11th day and there was no removed person for the next two days, the number of removed persons within the first 17 days was

limited. The estimated removed rate based on Siping epidemics is only suitable for the next few days and is not suitable for long-term prediction. We need to set the removed rate for long-term prediction. The population of Siping City is similar to that of Putian City, and the accumulative number of infected cases in this epidemic is close to that of Putian City. According to the introduction in Section 1, we can refer to the removed rate of Putian City as 0.003*t+0.01. To sum up, we set the removed rate $\gamma(t)$ of Siping City as $((a * t + b) * (H(19 - t) * H(t - 11)) + (0.003 * t + 0.01) * H(t - 19))$.

Yanbian Prefecture experienced two COVID-19 epidemics in a short period. For the first wave of COVID-19 epidemics, we use data from the first ten days for parameter estimations in the first wave. Since there are no removed persons in the first ten days, we set the removed rate according to the method described in Section 1. Since the population and the accumulative number of infected cases in Yanbian Prefecture are close to those in Putian City, we set the removed rate $\gamma(t)$ to (0.003t+0.01)*H(t-18). In addition, we set the transmission rate as an exponential decay function. In the second wave, we take the fifth-order moving average of the number of current infected and removed cases in the first 12 days and select the data of the first 11 days as parameter estimations. We set the transmission rate as a piecewise exponential decay function and the removed rate as an exponential increasing function.

The first wave of COVID-19 epidemics induced by the Omicron variant in Harbin City started on March 8th, 2022 and ended on April 8th, 2022. However, on April 13th, 2022, a new wave of COVID-19 epidemics occurred and ended on May 7th, 2022. We select data from the first twelve days for parameter estimations. Since there are few and irregular current removed persons in the first 12 days, we set the removed rate as H(t-18)*(0.005*t+0.02), according to the method introduced in Section 1. Prediction for the second wave of COVID-19 is influenced by the first wave. We can observe that the removed rate is an exponential decay function for the first eleven days and a linear increasing function after that time through the finite difference method. Consequently, the removed rate $\gamma(t)$ is $a * exp(b * t) * H(11 - t) + (c * t + d) * H(t - 11)$.

When the above three places are hit by the Omicron variant, Hohhot City was struck by the Delta variant. In order to test the validity of our model for epidemics induced by the Delta variant, we analyze the epidemic in Hohhot City. The only difference is that we set the average incubation period as 4 days. We use the method of the fifth-order moving average to process the accumulative number of the removed persons in the first 14 days and select the data of the first 13 days for parameter estimations. Estimated transmission and removed rates for Yanbian Prefecture and Siping, Harbin, and Hohhot cities are listed in Table 3. Because the number of susceptible persons is in the millions or more, the rate of transmission is very small. The model is sensitive to small changes in parameters. We need to keep as many bits as possible to ensure accurate parameters. Through strict epidemic prevention and control, the transmission rates gradually approach zero and the epidemic will be well controlled. The choice of the interval point for the transmission rate varies for different epidemics. For COVID-19 epidemics induced by the Omicron variant, the removed rate sometimes shows an exponential increase function, which is related to the fact that most of the infected people are asymptomatic. In some epidemics, the first removed person occurred late, and according to our introduction, it is an effective method to refer to the removed rate induced by the Delta variant. Strict epidemic prevention and control is an effective way to control the epidemic. Predictions of small-scale COVID-19 epidemics during the transmission of the Omicron variant in Yanbian Prefecture and Siping, Harbin, and Hohhot cities are presented in Figure 4.

Table 3. Parameter estimations for Yanbian Prefecture and Sping, Harbin, and Hohhot cities.

	$\beta(t)$	$\gamma(t)$
Siping City	$(H(14-t))*0.00000271999$ $*\exp(-0.38782697366t)+$ $(H(t-14))*0.00000017517$ $*\exp(-0.13023081804t)$	(H(19-t)H(t-11)) *(0.00132502090t-0.00997290728) +(0.003t+0.01)*H(t-19)
Yanbian Prefecture 1	$0.0000004722\exp(-0.16740135964t)$	(H(t-18))*(0.003*t+0.01)
Yanbian Prefecture 2	$(H(6-t))*0.00000073127$ $*\exp(-0.07792978146t)$ $+(H(t-6))*0.00000345277$ $*\exp(-0.43643698716t)$	(H(t-10))*0.00844930836 $*\exp(0.18757787171t)$
Harbin City 1	$(H(4-t))*0.00000013172$ $*\exp(-0.62452452759t)$ $+(H(t-4))*0.00000336186$ $*\exp(-0.35459855439t)$	(H(t-18))*(0.005t+0.02)
Harbin City 2	$(H(9-t))*0.00000005269$ $*\exp(0.02195607929t)$ $+(H(t-9))*0.00000017064$ $*\exp(-0.26120283487t)$	(H(11-t))*0.30985780310 $*\exp(-0.45512588013t)$ +(H(t-11)) *(0.01822215239t-0.21821698940)
Hohhot City	$(H(7-t))*0.00000407509$ $*\exp(-0.39425001193t)$ $+(H(t-7))*0.00000202093$ $*\exp(-0.34439849316t)$	(H(t-9))*0.00449537680 $*\exp(0.17026037510t)$

According to Table 4, we can obtain the following results. The predicted end times are the same as the actual end times in the first wave of the Harbin City epidemics and the Siping and Hohhot cities epidemics. In the second wave of epidemics in Harbin City, the predicted end time is 4 days away from the actual end time. In addition, the predicted end times of the first and second waves of the epidemics in Yanbian Prefecture are 16 days and 5 days away from the actual end times, respectively. For the maximum of current infected persons, the maximal relative error is only −6.82% in the first wave of COVID-19 in Yanbian Prefecture. The minimal relative error reaches −1.33% in Siping City. The relative errors of the epidemic in Hohhot City and the first wave of epidemics in Harbin City are 2.48% and 5.86%, respectively. Since the number of days of data used for parameter estimations exceeds the actual maximum time of current infected persons in the second waves of the epidemics in Yanbian Prefecture and Harbin City, we cannot estimate the maximum and its time of current infected persons. The predicted maximum times of current infected persons differ from the actual maximum times of current infected persons by the minimum of only one day in the first wave of epidemics in Harbin City

and the maximum of only four days in Siping City. The predicted maximum times of current infected persons differ from the actual maximum times of current infected persons by 2 days and 3 days in the epidemics in Hohhot City and the first wave of COVID-19 in Yanbian Prefecture, respectively. For the final size, there are very small relative errors of 0.66%, −0.35%, and 0.94%, respectively in the second wave of Harbin City epidemics and the Siping and Hohhot cities epidemics. The relative errors are 3.05% and −2.73% in the first and second waves of epidemics in Yanbian Prefecture, respectively. There is a large relative error of −10.22% due to the rebound at the end of the first epidemic in Harbin City.

The results indicate that the predicted indicators are very close to the actual indicators, implying that this model can be used to predict COVID-19 induced by not only the original strains and Delta strain, but also the Omicron strain very well.

Table 4. Comparisons of the predicted and actual maximum and maximum time of current infected persons, end time, and final size for Yanbian Prefecture and Siping, Harbin, and Hohhot cities, respectively.

	Siping City	Yanbian Prefecture 1	Yanbian Prefecture 2	Harbin City 1	Harbin City 2	Hohhot City
predicted end time	2022.4.18	2022.4.9	2022.5.3	2022.4.8	2022.5.11	2022.3.11
actual end time	2022.4.18	2022.3.24	2022.4.28	2022.4.8	2022.5.7	2022.3.11
predicted maximum of current infected persons	223	164	-	470	-	331
actual maximum of current infected persons	226	176	92	444	639	323
predicted maximum time of current infected persons	2022.3.30	2022.3.18	-	2022.3.25	-	2022.2.28
actual maximum time of current infected persons	2022.4.3	2022.3.21	2022.4.24	2022.3.26	2022.4.26	2022.2.26
predicted final size	281	203	107	536	764	431
actual final size	282	197	110	597	759	427

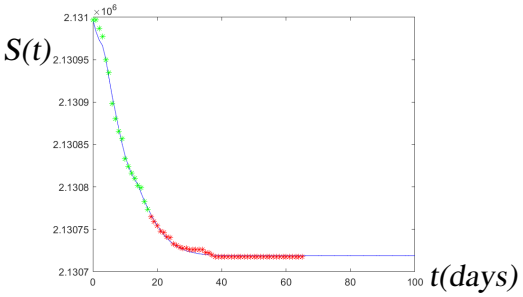

(a) Siping City

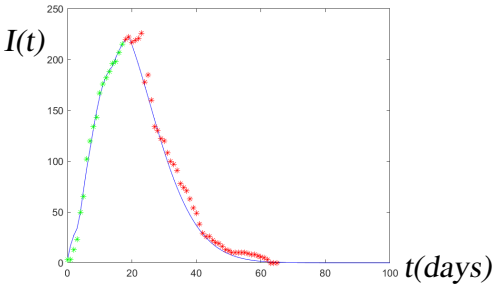

(b) Siping City

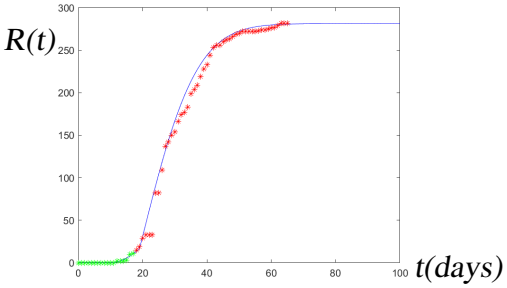

(c) Siping City

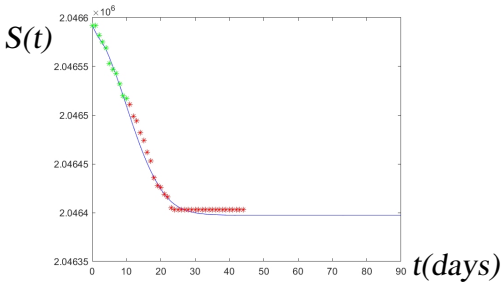

(d) Yanbian Prefecture 1

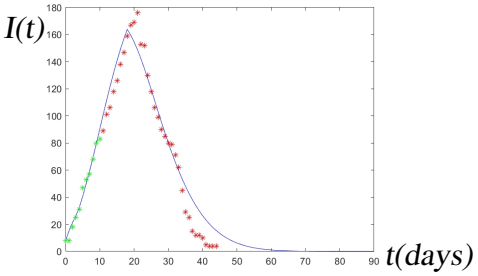

(e) Yanbian Prefecture 1

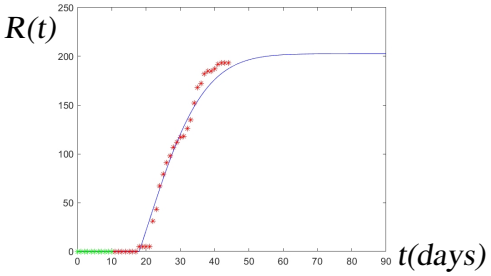

(f) Yanbian Prefecture 1

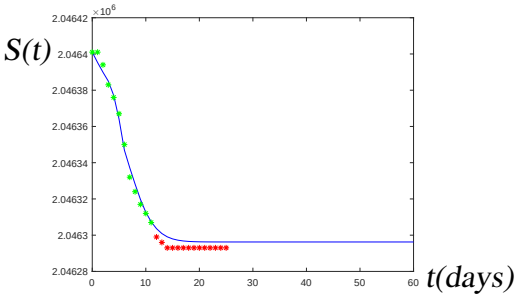

(g) Yanbian Prefecture 2

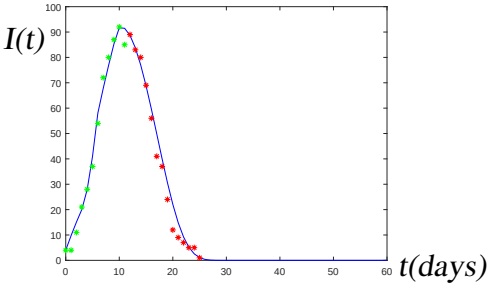

(h) Yanbian Prefecture 2

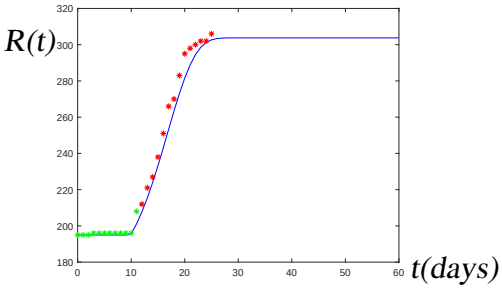

(i) Yanbian Prefecture 2

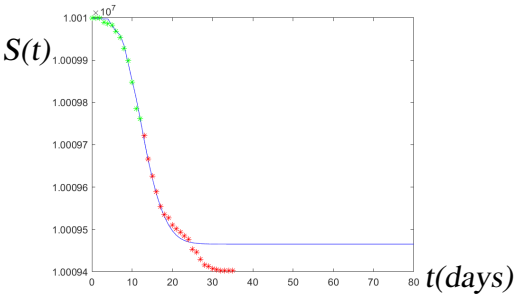

(j) Harbin City 1

Continued on next page

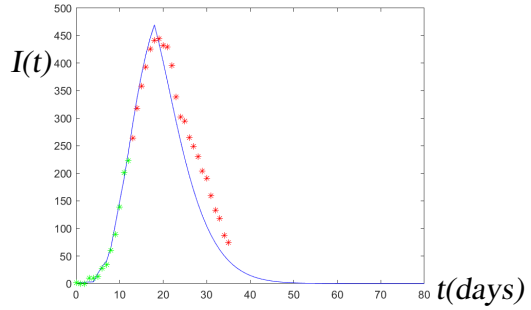

(k) Harbin City 1

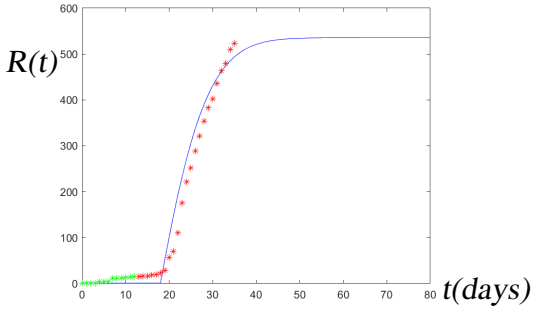

(l) Harbin City 1

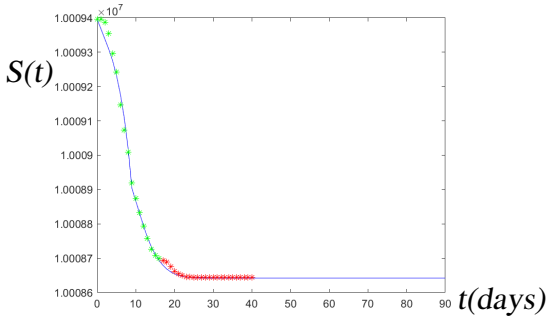

(m) Harbin City 2

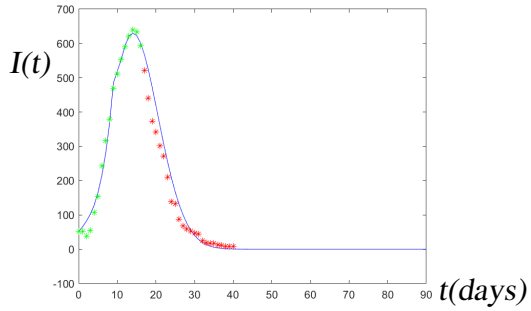

(n) Harbin City 2

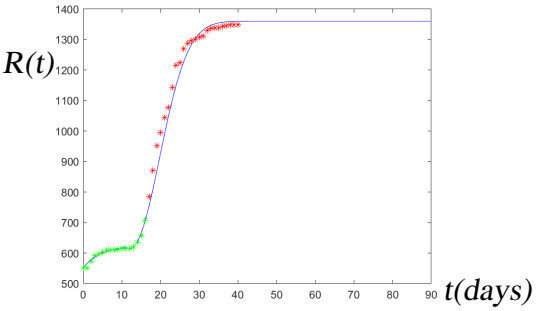

(o) Harbin City 2

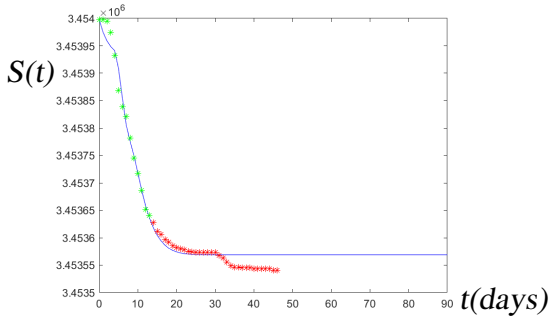

(p) Hohhot City

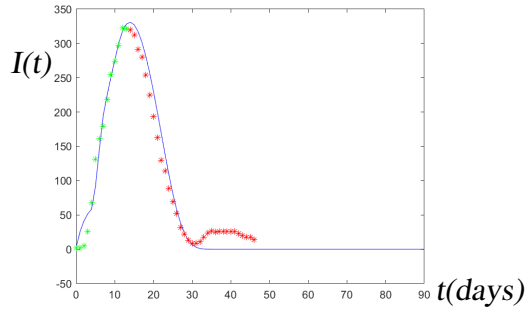

(q) Hohhot City

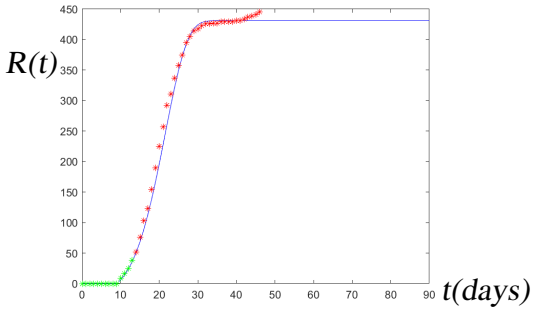

(r) Hohhot City

Figure 4. Predictions of small-scale COVID-19 epidemics during the transmission of the Omicron variant in Siping City (4a–4c), Yanbian Prefecture (4d–4i), Harbin City (4j–4o), and Hohhot City (4p–4r), where the green star represents the real data used for parameter estimation, the red star represents real data used for comparison with numerical simulations, and the solid line represents numerical simulations.

5. Predictions of large-scale COVID-19 epidemics during the transmission of the Omicron variant in China

Table 5. Start times and end times for epidemics in Jilin, Qingdao, Quanzhou, Binzhou, and Shanghai cities.

	Jilin City	Qingdao City	Quanzhou City	Binzhou City	Shanghai City
Start time	March 3rd, 2022	March 1st, 2022	March 13th, 2022	March 11th, 2022	May 26th, 2022
End time	May 11th, 2022	April 17th, 2022	April 15th, 2022	April 2nd, 2022	June 26th, 2022
Epidemic Strain	Omicron Variant	Omicron Variant	Omicron Variant	Omicron Variant	Omicron Variant

We predict large-scale epidemics in Jilin, Qingdao, Binzhou, and Quanzhou cities and fit the complex epidemic in Shanghai City. For the epidemic prediction in Jilin City, we select the data of the first 24 days for parameter estimations. Since the first removed person appeared on Day 21, we could not obtain accurate parameter estimations of the removed rate. Following the method proposed in Section 1, we set $\gamma(t)$, which is (a*t+b)*(H(27-t)*H(t-20))+(H(t-27))*(0.002*t+0.01).

For the epidemic prediction in Qingdao City, we select the data of the first 10 days for parameter estimations. Since there are no removed persons in the first ten days, we set the removed rate $\gamma(t)$, which is $(0.005 * t + 0.02) * H(t - 18)$, according to the method described in Section 1.

For the epidemic prediction in Quanzhou City, we use the method of the fifth-order moving average to process the accumulative number of the current infected and removed cases in the first 16 days and select the data of the first 16 days for parameter estimations.

For the epidemic prediction in Binzhou City, we use the method of the fifth-order moving average to process the accumulative number of infected persons in the first 14 days and select the data of the first 14 days for parameter estimations. Since there are no removed persons in the first 14 days, we set $\gamma(t)$, which is $(0.002 * t + 0.01) * H(t - 18)$, according to the method described in Section 1.

In Shanghai City, large-scale epidemic occurred in early March 2022. However, the statistics were not accurate enough due to poor monitoring for the epidemic. After the meeting of the Political Bureau of the Central Committee of the Communist Party of China on May 5th, 2022, strict controls were implemented in Shanghai City, and the statistics were realistic. Therefore, we started the statistics from that meeting onward. Additionally, the number of the current infected persons only includes confirmed cases and does not take into account asymptomatic cases, due to inaccurate statistics on asymptomatic infections. We choose May 26th, 2022 as the starting time of the epidemic and June 26th, 2022 as the end time. Due to the multiple rebounds in the epidemic, predicted results are undesirable. We only fit the epidemic. We use the method of the fifth-order moving average to process the number of the current accumulative infected and removed cases in the entire epidemic. Through the finite difference method, we can observe that $\beta(t)$ is no longer an exponential decay function but a piecewise quadratic function, which is $(k_1t^2 + k_2t + k_3) * H(13 - t) + (k_4t^2 + k_5t + k_6) * H(t - 13) * H(33 - t)$, and that $\gamma(t)$ is $(k_7 * \exp(k_8t)) * H(15 - t) + k_9 * H(t - 15)$. The initial parameters $k_1, k_2, k_3, \cdots, k_6$ are obtained

by quadratic polynomial fitting. The initial parameters k_7, k_8 are obtained by nonlinear fitting. The fitting results for Shanghai City are listed in Figure 5m–5o. Estimated transmission rates and removed rates for Jilin, Qingdao, Quanzhou, Binzhou, and Shanghai cities are listed in Table 6. Predictions of large-scale COVID-19 epidemics during the transmission of the Omicron variant in Jilin, Qingdao, Quanzhou, and Binzhou cities and fitting results for Shanghai City are presented in Figure 5.

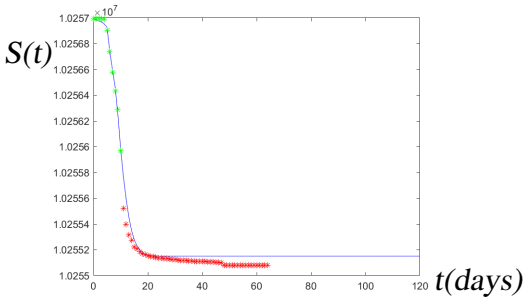

(a) Qingdao City

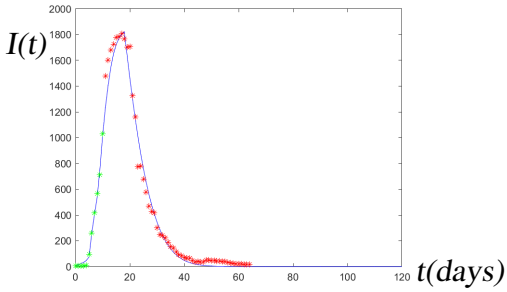

(b) Qingdao City

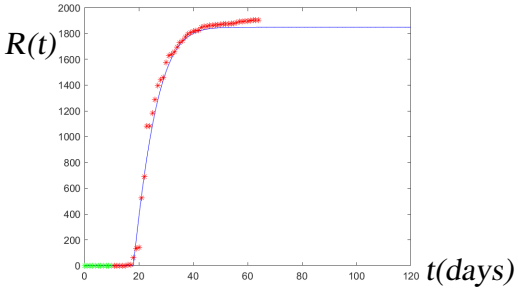

(c) Qingdao City

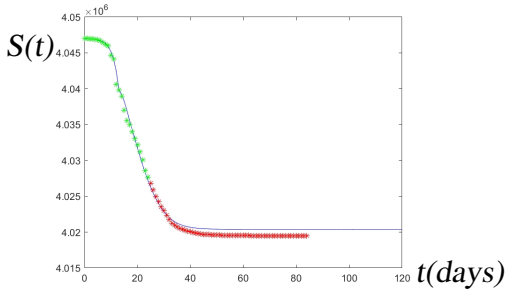

(d) Jilin City

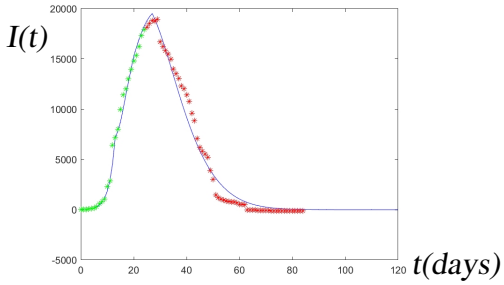

(e) Jilin City

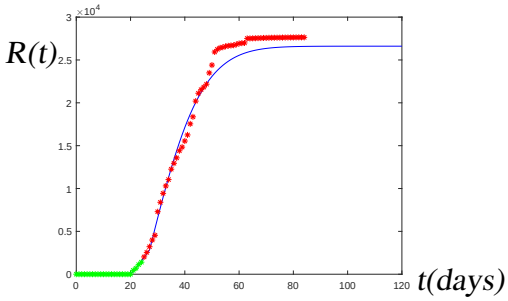

(f) Jilin City

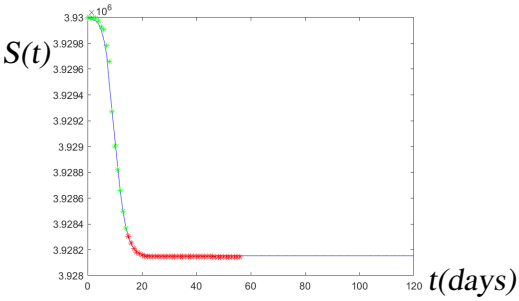

(g) Binzhou City

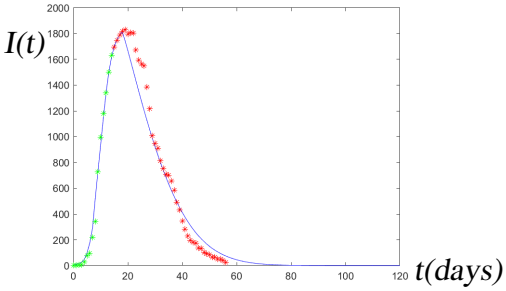

(h) Binzhou City

Continued on next page

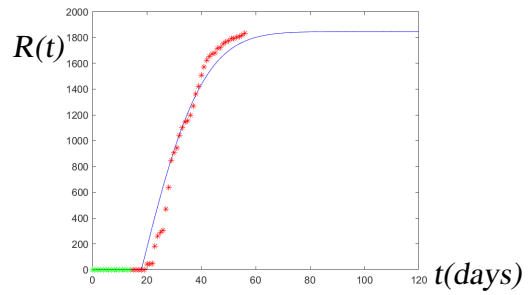

(i) Binzhou City

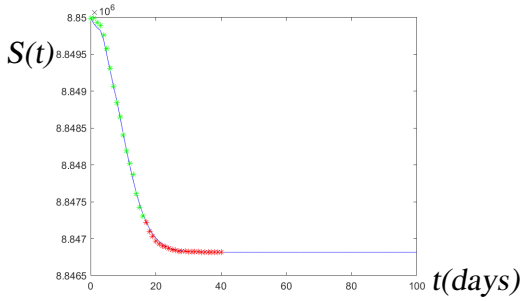

(j) Quanzhou City

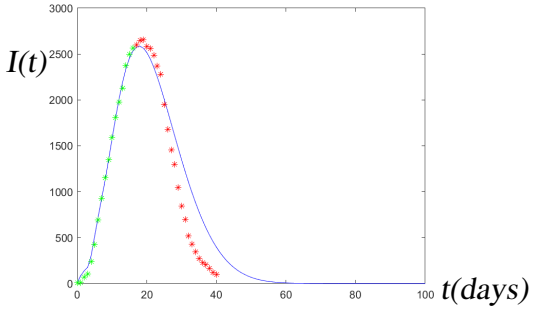

(k) Quanzhou City

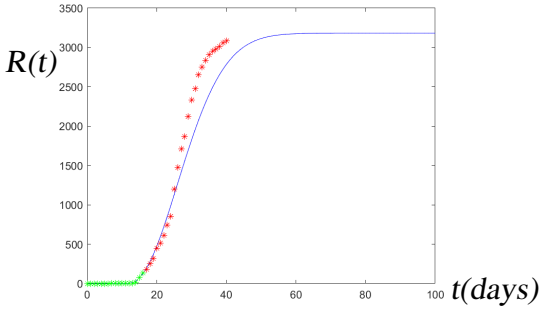

(l) Quanzhou City

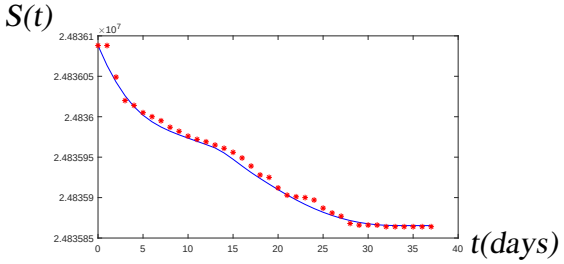

(m) Shanghai City

∗ real data - Numerical simulation

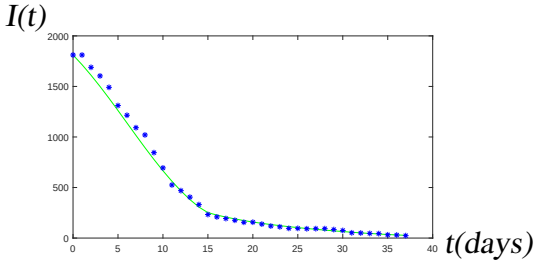

(n) Shanghai City

∗ real data - Numerical simulation

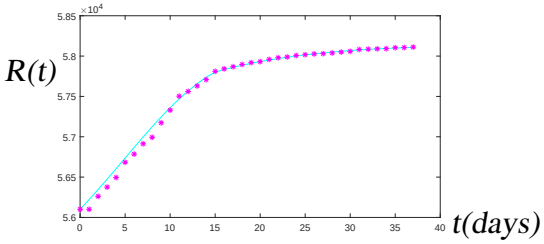

(o) Shanghai City

∗ real data - Numerical simulation

Figure 5. Predictions of large-scale COVID-19 epidemics during the transmission of the Omicron variant in Qingdao City (5a–5c), Jilin City (5d–5f), Binzhou City (5g–5i), and Quanzhou City (5j–5l) and fitting results for Shanghai City (5m–5o), where the green star represents the real data used for parameter estimation, the red star represents real data used for comparison with numerical simulations, and the solid line represents numerical simulations.

Table 6. Parameter estimations for Jilin, Qingdao, Quanzhou, Binzhou, and Shanghai cities.

	$\beta(t)$	$\gamma(t)$
Jilin City	$(H(13-t))*0.00000058058$ $*\exp(-0.02228400895t)$ $+(H(t-13))*0.00000053499$ $*\exp(-0.14857366023t)$	(0.00000013933t+0.02271890187) *(H(27-t)H(t-20)) +(0.002t+0.01)*H(t-27)
Qingdao City	$(H(5-t))*0.00000029747$ $*\exp(-0.18153338923t)$ $+(H(t-5))*0.00001162660$ $*\exp(-0.52972652027t)$	(0.005*t+0.02)*H(t-18)
Quanzhou City	$(H(7-t))*0.00000101521$ $*\exp(-0.34959309604t)$ $+(H(t-7))*0.00000034370$ $*\exp(-0.25079426027t)$	(0.00523610709t-0.06006439954) *H(t-12)
Binzhou City	$(H(8-t))*0.00000106470$ $*\exp(-0.03528409187t)$ $+(H(t-8))*0.00003572880$ $*\exp(-0.52897238030t)$	(0.002t+0.01)*H(t-18)
Shanghai City	$(5.8*10^{-12}t^2-1.017*10^{-10}t$ $+5.945*10^{-10})*H(13-t)$ $+(-1.2*10^{-11}t^2+5.38*10^{-10}t$ $-4.66*10^{-9})*H(t-13)$ $*H(33-t)$	$0.065*\exp(0.0949t)$ $*H(15-t)$ $+0.12852764455*H(t-15)$

Table 7. Comparisons of actual and predicted maximum and its time of current infected persons, end time, and final size for Jilin, Qingdao, Quanzhou, and Binzhou cities, respectively.

	Jilin City	Qingdao City	Quanzhou City	Binzhou City
predicted end time	2022.5.12	2022.3.24	2022.4.20	2022.4.4
actual end time	2022.5.11	2022.4.17	2022.4.15	2022.4.2
predicted maximum of current infected persons	19,521	1821	2585	1813
actual maximum of current infected persons	18,933	1808	2653	1829
predicted maximum time of current infected persons	2022.3.29	2022.3.18	2022.3.30	2022.3.28
actual maximum time of current infected persons	2022.3.31	2022.3.17	2022.3.31	2022.3.29
predicted final size	26,609	1849	3182	1846
actual final size	27,499	1920	3180	1857

According to Table 7, we can obtain the following results. The predicted end time is only one day away from the actual end time in Jilin City, which is the best result. The predicted end times of the epidemics in Binzhou and Quanzhou cities are 2 days and 5 days away from the actual end times, respectively. The predicted end time is 24 days away from the real end time, as sporadic cases continued to appear in Qingdao City near the end of the epidemic. For the maximum of current infected persons, there are very small relative errors of -0.87% and 0.72% in Binzhou and Qingdao cities. In Jilin and Quanzhou cites, the relative errors are 3.11% and -2.56%, respectively. For the maximum time of current infected persons, predicted results are excellent. The predicted maximum times of current infected persons differ from the actual maximum times of current infected persons by no more than two days in these four cities. For the final size, the perfect result is a difference of two persons in Quanzhou City. There is a very small relative error of -0.59% in Binzhou City. The relative errors are -3.70% and -3.24% in Qingdao and Jilin cities.

All in all, the indicators we predict are very close to the actual ones. For the predictions of large-scale COVID-19 epidemics, our approach remains simple but effective.

6. Conclusions and discussion

This paper contributes to the prediction of COVID-19 epidemics induced by the Omicron variant. It verifies the effectiveness of the time-delayed SIR model for COVID-19 epidemics induced by the Omicron variant. We apply a NATD-SIR model to make predictions of the present susceptible, infected, and removed persons in COVID-19 epidemics during the transmission of the Omicron variant and obtain good prediction results. We develop an accurate prediction method for complex COVID-19 epidemics during the transmission of the Omicron variant. Accurate fitting methods are established for very complex large-scale COVID-19 epidemics induced by the Omicron variant. The incubation period of the Omicron variant is shorter than that of the Delta variant. We set the average incubation period for the Delta variant to be 4 days and for the Omicron variant to be 3 days.

The innovations of this paper are the following:

- By the finite difference method, it has been observed that $\beta(t)$ is approximately an exponential decay function. In Shanghai City, $\beta(t)$ is approximately a piecewise quadratic function. Since the epidemic induced by the Omicron variant lasts longer, it is necessary to choose more initial days for parameter estimations. Instead of using a simple exponential decay function, a piecewise exponential decay function is chosen to estimate the transmission rates. By this way, we can get more accurate parameter estimations of transmission rates in the epidemic induced by the Omicron variant. $\gamma(t)$ is approximately (a*t+b)*H(t-k) (a>0). In a few epidemics, $\gamma(t)$ is approximately equal to an exponential increasing function.
- In addition, we analyze removed rates of COVID-19 epidemics induced by the Delta variant and the Omicron variant in different regions. It is found that the removed rates of epidemics may be similar in regions with similar populations and final sizes no matter whether they are induced by the Delta variant or the Omicron variant. If two regions have similar populations, the region with a higher number of infected persons may have a lower removed rate. Sometimes, we cannot estimate parameters of removed rates since there are no removed persons or too few removed persons in the initial days in some regions. We can refer to the removed rates of COVID-19 epidemics induced by the Delta variant in [18]. In this way, we can predict the COVID-19 epidemics with less data.
- The daily number of newly-increased infected and removed persons can sometimes vary greatly. This can lead to larger or smaller parameter estimations of transmission and removed rates. To mitigate this, we take the fifth-order moving average to preprocess the number of the current accumulative infected or removed persons. By this way, we can obtain more accurate parameter estimations. Our predicted indicators are close to the actual ones for the maximum and its time of current infected persons, end time, and final size. Based on these indicators, we can provide valuable references and suggestions for epidemic prevention and control, resumption of work, production, and school.

The reason for the inadequate prediction of the COVID-19 epidemic in some regions is related to the characteristics of the Omicron epidemic: highly contagious, spreading quickly, and more concealed. In addition, some published epidemic data is inaccurate. They greatly increase the difficulty of epidemic prediction. There are some shortcomings here. Because we need to estimate accurate transmission and removed rates, we often choose more epidemic data, sometimes exceeding the time of the peak, which will reduce the effect of practical application. Additionally, the relationship between removed rates across the epidemic still needs to be explored. If there is a rebound in the epidemic, the forecast of the overall epidemic will be biased.

In the future, we have some plans in the following:

- We can consider the time-delay of removed persons, since it takes an amount of time for an infected person to become a removed person.
- For data preprocessing, we just perform a simple fifth-order moving average. Other processing methods can also be tried.
- Many machine learning methods can be used for COVID-19 prediction. Machine learning can be studied to make accurate short-term predictions, adding the results of the predictions to the data used for parameter estimation and, therefore, obtaining more accurate parameters estimation with

fewer data.

- We compare the transmission rates of different epidemics and found no significant relationship between transmission rates and regional population, duration, or number of infected cases. We still need to explore this aspect.

Use of AI tools declaration

The authors declare they have not used Artificial Intelligence (AI) tools in the creation of this article.

Acknowledgments

The authors would like to acknowledge the financial support for this research via the National Natural Science Foundation of China (Nos. 11972327 and 11372282) and National College Students' Innovation and Entrepreneurship Training Program of China (No. 202210459015). They also thank the reviewers for their valuable reviews and kind suggestions.

Conflict of interest

The authors declare there are no conflicts of interest.

References

1. S. Y. Ren, W. B. Wang, R. D. Gao, A. M. Zhou, Omicron variant (B. 1.1. 529) of SARS-CoV-2: mutation, infectivity, transmission, and vaccine resistance, *World J. Clin. Cases*, **10** (2022), 1–11. https://doi.org/10.12998/wjcc.v10.i1.1
2. L. Lu, B. W. Y. Mok, L. L. Chen, J. M. C. Chan, O. T. Y. Tsang, B. H. S. Lam, et al., Neutralization of severe acute respiratory syndrome coronavirus 2 omicron variant by sera from BNT162b2 or CoronaVac vaccine recipients, *Clin. Infect. Dis.*, **75** (2022), e822–e826. https://doi.org/10.1093/cid/ciab1041
3. H. F. Tseng, B. K. Ackerson, Y. Luo, L. S. Sy, C. A. Talarico, Y. Tian, et al., Effectiveness of mRNA-1273 against SARS-CoV-2 Omicron and Delta variants, *Nat. Med.*, **28** (2022), 1063–1071. https://doi.org/10.1038/s41591-022-01753-y
4. W. O. Kermack, A. G. McKendrick, A contribution to the mathematical theory of epidemics, *Proc. R. Soc. A*, **115** (1927), 700–721. https://doi.org/10.1098/rspa.1927.0118
5. K. L. Cooke, Stability analysis for a vector disease model, *Rocky Mountain J. Math.*, **9** (1979), 31–42. https://doi.org/10.1216/RMJ-1979-9-1-31
6. N. Guglielmi, E. Iacomini, A. Viguerie, Delay differential equations for the spatially resolved simulation of epidemics with specific application to COVID-19, *Math. Methods Appl. Sci.*, **45** (2022), 4752–4771. https://doi.org/10.1002/mma.8068
7. L. Dell'Anna, Solvable delay model for epidemic spreading: the case of COVID-19 in Italy, *Sci. Rep.*, **10** (2020), 15763. https://doi.org/10.1038/s41598-020-72529-y

8. I. Rahimi, F. Chen, A. H. Gandomi, A review on COVID-19 forecasting models, *Neural Comput. Appl.*, **35** (2023), 23671–23681. https://doi.org/10.1007/s00521-020-05626-8
9. Z. Lv, J. Zeng, Y. Ding, X. Liu, Stability analysis of time-delayed SAIR model for duration of vaccine in the context of temporary immunity for COVID-19 situation, *Electron. Res. Arch.*, **31** (2023), 1004–1030. https://doi.org/10.3934/era.2023050
10. Y. Mohamadou, A. Halidou, P. T. Kapen, A review of mathematical modeling, artificial intelligence and datasets used in the study, prediction and management of COVID-19, *Appl. Intell.*, **50** (2020), 3913–3925. https://doi.org/10.1007/s10489-020-01770-9
11. T. T. Marinov, R. S. Marinova, Dynamics of COVID-19 using inverse problem for coefficient identification in SIR epidemic models, *Chaos, Solitons Fractals:X*, **5** (2020), 100041. https://doi.org/10.1016/j.csfx.2020.100041
12. M. Karim, A. Kouidere, M. Rachik, K. Shah, T. Abdeljawad, Inverse problem to elaborate and control the spread of COVID-19: a case study from Morocco, *AIMS Math.*, **8** (2023), 23500–23518. https://doi.org/10.3934/math.20231194
13. A. Comunian, R. Gaburro, M. Giudici, Inversion of a SIR-based model: a critical analysis about the application to COVID-19 epidemic, *Physica D*, **413** (2020), 132674. https://doi.org/10.1016/j.physd.2020.132674
14. I. Cooper, A. Mondal, C. G. Antonopoulos, A SIR model assumption for the spread of COVID-19 in different communities, *Chaos, Solitons Fractals*, **139** (2020), 110057. https://doi.org/10.1016/j.chaos.2020.110057
15. F. S. Lobato, G. M. Platt, G. B. Libotte, A. J. S. NETO, Formulation and solution of an inverse reliability problem to simulate the dynamic behavior of COVID-19 pandemic, *Trends Comput. Appl. Math.*, **22** (2021), 91–107. https://doi.org/10.5540/tcam.2021.022.01.00091
16. C. C. Pacheco, C. R. de Lacerda, Function estimation and regularization in the SIRD model applied to the COVID-19 pandemics, *Inverse Probl. Sci. Eng.*, **29** (2021), 1613–1628. https://doi.org/10.1080/17415977.2021.1872563
17. F. S. Lobato, G. B. Libotte, G. M. Platt, Identification of an epidemiological model to simulate the COVID-19 epidemic using robust multiobjective optimization and stochastic fractal search, *Comput. Math. Methods Med.*, **2020** (2020), 9214159. https://doi.org/10.1155/2020/9214159
18. L. J. Pei, Y. H. Hu, Long-term prediction of the sporadic COVID-19 epidemics induced by δ-virus in China based on a novel non-autonomous delayed SIR model, *Eur. Phys. J. Spec. Top.*, **231** (2022), 3649–3662. https://doi.org/10.1140/epjs/s11734-022-00622-6
19. L. J. Pei, M. Y. Zhang, Long-term predictions of current confirmed and dead cases of COVID-19 in China by the non-autonomous delayed epidemic models, *Cognit. Neurodyn.*, **16** (2022), 229–238. https://doi.org/10.1007/s11571-021-09701-1
20. L. J. Pei, M. Y. Zhang, Long-term predictions of COVID-19 in some countries by the SIRD model, *Complexity*, **2021** (2021), 6692678. https://doi.org/10.1155/2021/6692678

21. H. Jahanshahi, J. M. Munoz-Pacheco, S. Bekiros, N. D. Alotaibi, A fractional-order SIRD model with time-dependent memory indexes for encompassing the multi-fractional characteristics of the COVID-19, *Chaos, Solitons Fractals*, **143** (2021), 110632. https://doi.org/10.1016/j.chaos.2020.110632

22. C. Anastassopoulou, L. Russo, A. Tsakris, C. Siettos, Data-based analysis, modelling and forecasting of the COVID-19 outbreak, *PLoS One*, **15** (2020), e0230405. https://doi.org/10.1371/journal.pone.0230405

23. S. He, Y. X. Peng, K. H. Sun, SEIR modeling of the COVID-19 and its dynamics, *Nonlinear Dyn.*, **101** (2020), 1667–1680. https://doi.org/10.1007/s11071-020-05743-y

24. Z. Yang, Z. Q. Zeng, K. Wang, S. S. Wong, W. Liang, M. Zanin, et al., Modified SEIR and AI prediction of the epidemics trend of COVID-19 in China under public health interventions, *J. Thoracic Dis.*, **12** (2020), 165–174. https://doi.org/10.21037/jtd.2020.02.64

25. S. Annas, M. I. Pratama, M. Rifandi, W. Sanusi, S. Side, Stability analysis and numerical simulation of SEIR model for pandemic COVID-19 spread in Indonesia, *Chaos, Solitons Fractals*, **139** (2020), 110072. https://doi.org/10.1016/j.chaos.2020.110072

26. R. Engbert, M. M. Rabe, R. Kliegl, S. Reich, Sequential data assimilation of the stochastic SEIR epidemic model for regional COVID-19 dynamics, *Bull. Math. Biol.*, **83** (2021), 1. https://doi.org/10.1007/s11538-020-00834-8

27. S. Margenov, N. Popivanov, I. Ugrinova, S. Harizanov, T. Hristov, Mathematical and computer modeling of COVID-19 transmission dynamics in Bulgaria by time-depended inverse SEIR model, *AIP Conf. Proc.*, **2333** (2021), 090024. https://doi.org/10.1063/5.0041868

28. E. Li, Q. Zhang, Global dynamics of an endemic disease model with vaccination: analysis of the asymptomatic and symptomatic groups in complex networks, *Electron. Res. Arch.*, **31** (2023), 6481–6504. https://doi.org/10.3934/era.2023328

29. G. Fan, N. Li, Application and analysis of a model with environmental transmission in a periodic environment, *Electron. Res. Arch.*, **31** (2023), 5815–5844. https://doi.org/10.3934/era.2023296

30. W. P. Jia, K. Han, Y. Song, W. Z. Cao, S. S. Wang, S. S. Yang, et al., Extended SIR prediction of the epidemics trend of COVID-19 in Italy and compared with Hunan, China, *Front. Med.*, **7** (2020), 169. https://doi.org/10.3389/fmed.2020.00169

31. M. Turkyilmazoglu, An extended epidemic model with vaccination: weak-immune SIRVI, *Physica A*, **598** (2022), 127429. https://doi.org/10.1016/j.physa.2022.127429

32. C. Iwendi, A. K. Bashir, A. Peshkar, R. Sujatha, J. M. Chatterjee, S. Pasupuleti, et al., COVID-19 patient health prediction using boosted random forest algorithm, *Front. Public Health*, **8** (2020), 357. https://doi.org/10.3389/fpubh.2020.00357

33. G. Pinter, I. Felde, A. Mosavi, P. Ghamisi, R. Gloaguen, COVID-19 pandemic prediction for hungary; a hybrid machinelearning approach, *Mathematics*, **8** (2020), 890. https://doi.org/10.3390/math8060890

34. M. Zivkovic, N. Bacanin, K. Venkatachalam, A. Nayyar, A. Djordjevic, I. Strumberger, et al., COVID-19 cases prediction by using hybrid machine learning and beetle antennae search approach, *Sustainable Cities Soc.*, **66** (2021), 102669. https://doi.org/10.1016/j.scs.2020.102669

35. A. S. Kwekha-Rashid, H. N. Abduljabbar, B. Alhayani, Coronavirus disease (COVID-19) cases analysis using machine learning applications, *Appl. Nanosci.*, **13** (2023), 2013–2015. https://doi.org/10.1007/s13204-021-01868-7

36. F. Rustam, A. A. Reshi, A. Mehmood, S. Ullah, B. W. On, W. Aslam, et al., COVID-19 future forecasting using supervised machine learning models, *IEEE Access*, **8** (2020), 101489–101499. https://doi.org/10.1109/ACCESS.2020.2997311

37. R. Salgotra, M. Gandomi, A. H. Gandomi, Time series analysis and forecast of the COVID-19 pandemic in India using genetic programming, *Chaos, Solitons Fractals*, **138** (2020), 109945. https://doi.org/10.1016/j.chaos.2020.109945

38. H. Abbasimehr, R. Paki, Prediction of COVID-19 confirmed cases combining deep learning methods and Bayesian optimization, *Chaos, Solitons Fractals*, **142** (2021), 110511. https://doi.org/10.1016/j.chaos.2020.110511

39. M. Turkyilmazoglu, A highly accurate peak time formula of epidemic outbreak from the SIR model, *Chin. J. Phys.*, **84** (2023), 39–50. https://doi.org/10.1016/j.cjph.2023.05.009

40. M. Turkyilmazoglu, Explicit formulae for the peak time of an epidemic from the SIR model, *Physica D*, **422** (2021), 132902. https://doi.org/10.1016/j.physd.2021.132902

41. Z. Guo, S. Zhao, C. K. P. Mok, R. T. Y. So, C. H. K. Yam, T. Y. Chow, et al., Comparing the incubation period, serial interval, and infectiousness profile between SARS-CoV-2 Omicron and Delta variants, *J. Med. Virol.*, **95** (2023), e28648. https://doi.org/10.1002/jmv.28648

AIMS Press